

Supporting Information

Genetic Circuit Performance Under Conditions Relevant for Industrial Bioreactors *Moser et al.*

Table of Contents

- I. Circuit performance and impact on growth in shake flask experiments**
 - I.A. Impact of gates on cell growth*
 - I.B. Population behavior of gates in various culture conditions*
 - I.C. Population behavior of the AND gate with different RBSs*

- II. RBS Performance is consistent across strain and media**

- III. Detailed microreactor data**

- IV. Performance of an AND gate during fermentation**

- V. Plasmid retention in the 10 L bioreactor**

- VI. Relative Expression Unit (REU) Conversions**

- VII. Variations and Parameters of Individual 10 L Bioreactor Runs**
 - VII.A. Run #1: AND gate in E. coli DH10B with different amounts of yeast extract*
 - VII.B. Run #2: AND gate in E. coli DS68637 with different amounts of yeast extract*
 - VII.C. Run #3: AND gate RBS variants in E. coli DS68637*
 - VII.D. Run #4: AND gates and the reference plasmid in E. coli DS68637*

- VIII. Genetic Parts and Plasmids**

- IX. Supplementary References**

I. Circuit performance and impact on growth in shake flask experiments

I.A. Impact of gates on cell growth

Figures 2 and 3 in the main text show the performance of the AND/NOR gates across different media and strains. The corresponding impact on cell growth of these different conditions and gate activation is shown below. Figure S1 shows how growth is impacted by media for *E. coli* DH10B cells. Both gates show higher final cell densities with increased amount of supplement in the media, and the addition of inducers reduced growth for both gates. Figure S2 shows that this effect is present across different strains and media, though DS68637[†] grows to higher densities than DH10B.

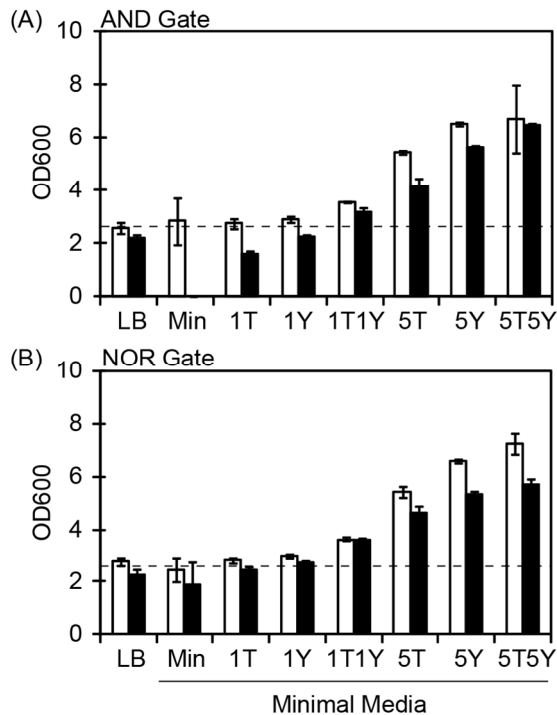
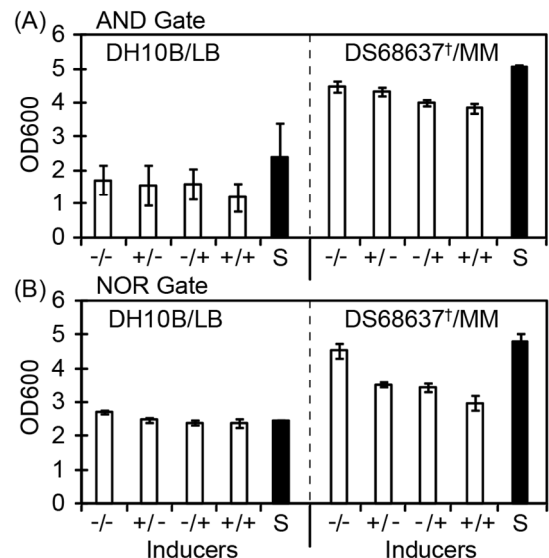


Figure S1: Impact of the circuit and media on growth. The data corresponds to the experiments in Figure 2 and the media compositions are described in that figure. The final OD₆₀₀ of the culture is shown for (A) the AND gate and (B) the NOR gate in *E. coli* DH10B. The data is shown for uninduced (white bars) and fully induced (black bars) cultures. All cultures were measured after 9 hours, except the cultures that were grown on unsupplemented minimal medium (Min), which were measured after 24 hours. Induced AND gates did not grow on unsupplemented minimal media (Min). The dashed line is the mean OD₆₀₀ of the reference plasmid (pFM46) grown in DH10B in LB after 9 hours.

Figure S2: Growth of different *E. coli* strains carrying the gates. The data corresponds to Figure 3. (A) The OD₆₀₀ of the AND gate is shown for four combinations of inputs: -/- (no inducers), +/- (1.3 mM arabinose), -/+ (0.63 mM salicylate), and +/+ (both inducers). (B) The OD₆₀₀ of the NOR gate cultures is shown for four combinations of inputs: -/- (no inducers), +/- (1.3 mM arabinose), -/+ (100 ng/ml aTc), and +/+ (both inducers). The OD₆₀₀ of the reference plasmid pFM46 (S) is shown. In DH10B, the AND gates were measured after 9 hours and NOR gates were measured after 24 hours. In DS68637[†] on Minimal medium (MM), the AND and the NOR gate were both measured after 24 hours.



I.B. Population behavior of gates under various culture conditions

The data shown in Figure 2 of the main text are the geometric means of the fluorescence of a culture, as measured by flow cytometry. The complete distributions are provided here to show the variability in the populations. In Figure S3, the population variability of the two gates is shown for the uninduced and induced conditions. The ON state of the AND gate is very media dependent, whereas both the ON and OFF states of the NOR gate are robust across media.

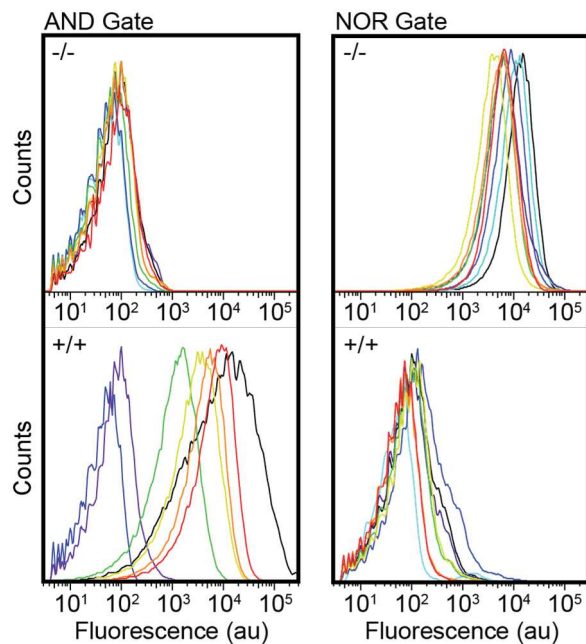


Figure S3: Cytometry distributions for AND and NOR gates in *E. coli* DH10B. The distributions are representative of the data shown in Figure 2. Each culture is color coded for the media: LB (black), minimal medium (light blue), 1T (dark blue), 1Y (purple), 1T1Y (green), 5T (yellow), 5Y (orange), 5T5Y (red), where the number before the letter refers to the amount in g/L, T refers to tryptone, and Y refers to yeast extract. The uninduced (-/-) and induced (+/+) data are shown in the top and bottom graphs, respectively.

I.C. Population behavior of the AND gate with different RBSs

Ribosome Binding Sites (RBSs) of different strength were chosen to connect the arabinose-inducible promoter to the AND gate. Differences in performance of these AND gate variants was shown for shake flask experiments (Figure 5) and 10 L fermentors (Figures 7). Here, the raw cytometry distributions are provided for the shake flask experiments. The distributions show that the weaker RBS variants (RBS_C and RBS_D) often exhibit skewed or multimodal distributions. RBS_B is the variant that is tested in the shake flask cultures and the microreactor (Figures 3, 4, 6, S1, S2, S3).

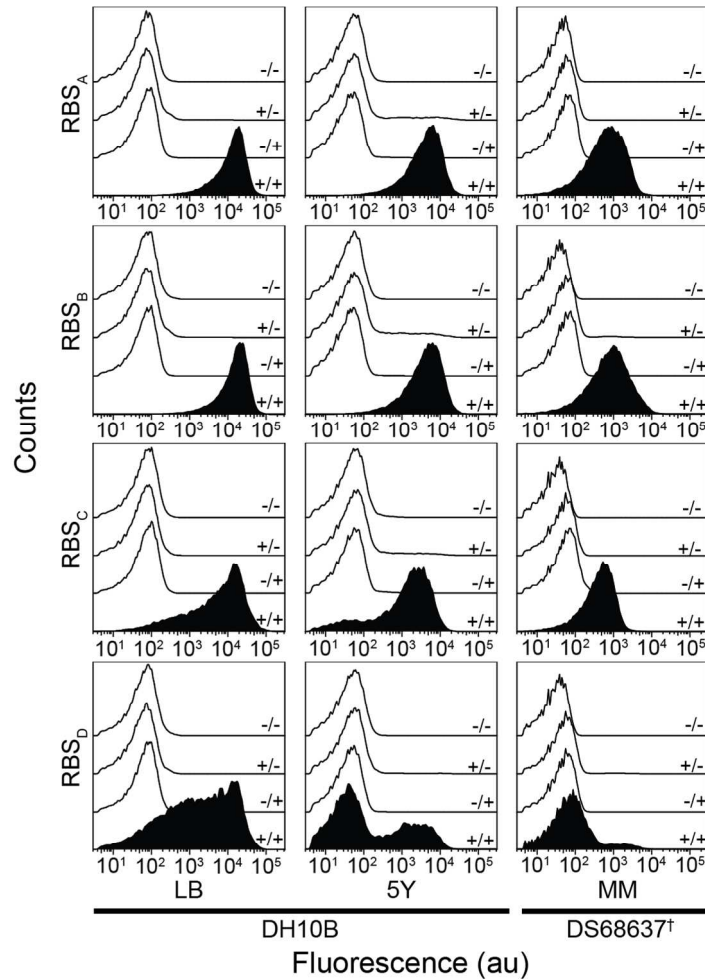
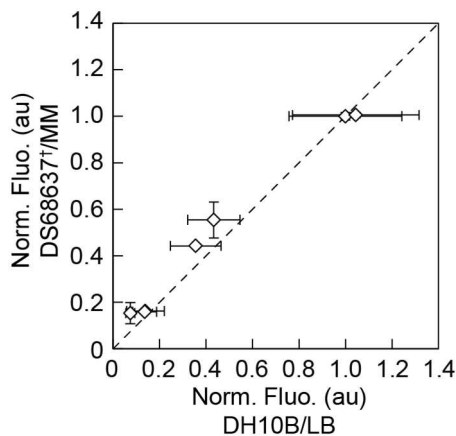


Figure S4: Cytometry distributions of different RBS variants. The distributions are representative of the data used to calculate the averages in Figure 4. The gates were grown with either no inducer (-/-), 1.3 mM arabinose (+/-), 0.63 mM salicylate (-/+), or both inducers (+/+). DH10B were grown in LB and minimal medium with 5 g/L yeast extract (5YE). DS68637⁺ were grown in minimal medium (MM).

II. RBS Performance is consistent across strain and media



RBSs are commonly used to tune genetic circuits and were used here to tune AND gate performance. To test if RBS strength changes with different media and strains, we grew DH10B and DS68637⁺ containing plasmids that constitutively expressed RFP from different strength RBSs (pFM169-174, Table S3). Each RBS performed similarly across different strain and media contexts.

Figure S5: RBS performance in different strains/media.

A collection of engineered RBSs (FwEng 1, 2, 5, 6, 11, 14; Table S2) was measured in DH10B in LB and in DS68637⁺ in minimal medium (MM) in shake flasks. Fluorescence of each construct was normalized to the strongest construct in the series. RBS performance was consistent ($R^2 = 0.964$) across both media and strains.

III. Detailed microreactor data

We grew an AND gate and the reference plasmid pFM46 in DS68637 in a BioLector microreactor to test gate performance.⁷ Relative culture density was measured by light scatter and is reported in arbitrary units (au). Fluorescence was measured by spectrophotometry with an excitation at 486 nm and emission at 510 nm. pH was measured via an optode that excited at 486 nm and emitted at 530 nm. Dissolved oxygen was measured via an optode that excited at 505 nm and emitted at 590 nm. Dissolved oxygen was maintained at maximal saturation to maintain growth through carbon limitation. The culture was grown under 80% humidity control at 30 °C at 1000 RPM elliptical shaking.

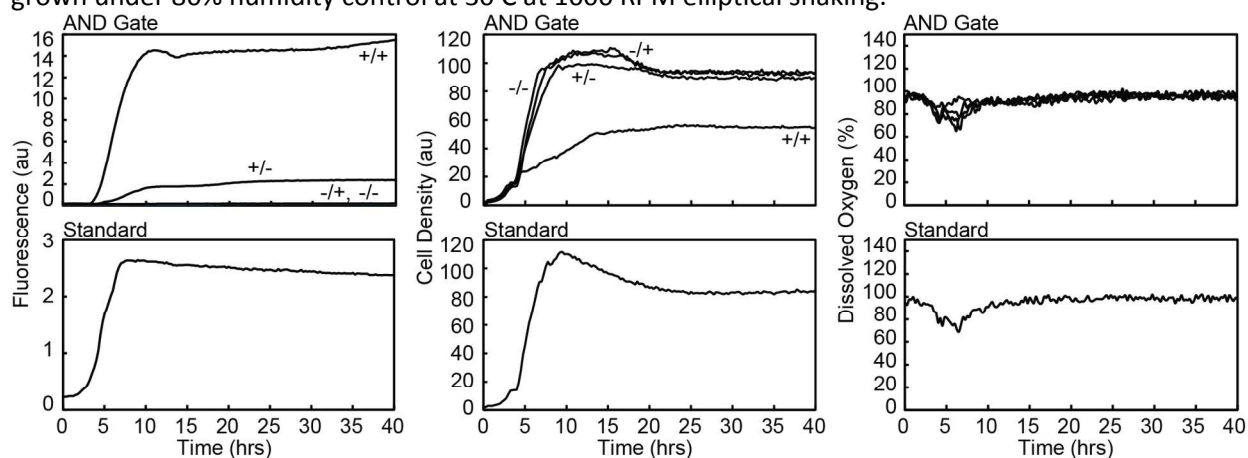


Figure S6: Raw fluorescence, growth, and oxygen content of the gates and reference plasmid in the microreactor. The RBS_B AND gate and the reference plasmid (pFM46, “Standard”) were grown in 1 ml batch of rich 2xYT media in the presence of either no inducers (-/-), single inducers (-/+), arabinose only (+/-), salicylate only (-/+), or both inducers (+/+).

IV. Performance of an AND gate during fermentation

To determine the effect of yeast extract on AND gate function in DS68637, we grew DS68637 carrying the RBS_B AND gate in a 10 L fermentor with 0 or 20 g/L of yeast extract in the glucose feed. In DH10B, 100 g/L were required in the feed for the AND gate to function (Figure 7). In DS68637, the AND gate functioned without any yeast extract added to the feed, and performed identically with and without yeast extract in the feed (Figure S7A).

To compare the performance of the AND gate directly to a reference plasmid, we grew DS68637 carrying the AND gate or the reference plasmid in a 10 L bioreactor. We induced the AND gate in reverse order than in previous fermentations to examine the arabinose-only state of the gate. The AND gate functioned fully upon only arabinose induction, indicating a failure to carry out the correct computation. The reference plasmid maintained a fairly constant level of fluorescence throughout growth (Figure S7B).

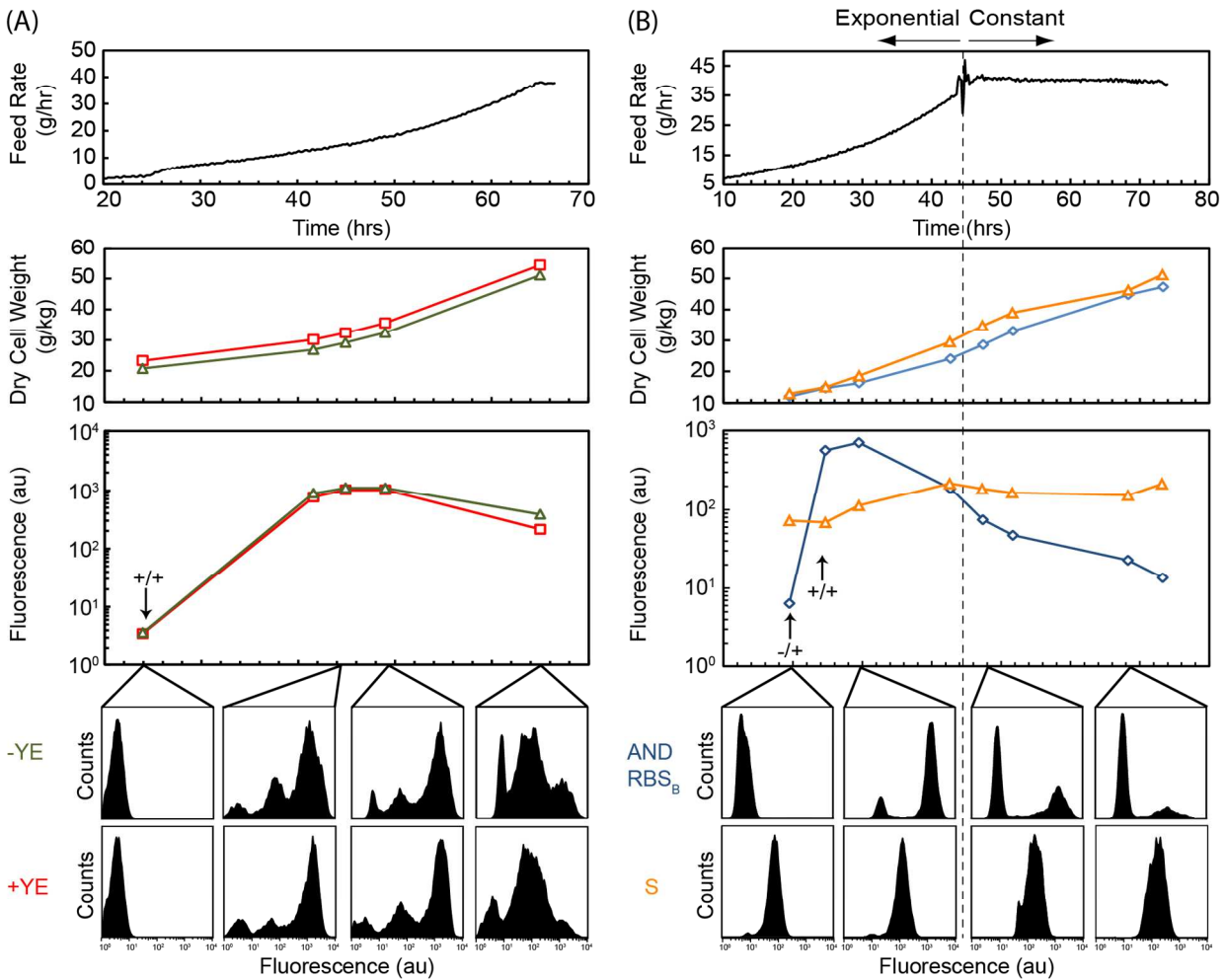


Figure S7: Additional states of the AND gate in a 10 L bioreactor.

(A) Data from Runs # 4 and 5 (Table S1), the growth of the RBS_C AND gate in DS68637 with and without 20 g/L yeast extract in the feed (+YE and -YE, respectively). The gate performs identically in both conditions. (B) Data from Runs # 9 and 10 (Table S1), the growth of the RBS_B AND gate and the reference plasmid (pFM46). The data for the reference plasmid (S) is identical to that shown in Fig. 7 of the main text. The AND gate is induced first with arabinose at 22 hours (-/+) and then with salicylate 3 hours later (+/+). The AND gate was fully induced after addition of only arabinose, representing a failure mode of the gate. The reference plasmid shows consistent fluorescence throughout growth, even after switch to constant feeding. The cytometry distributions of the AND gate resemble those from previous fermentations and show a multimodal distribution following cessation of the exponential feed.

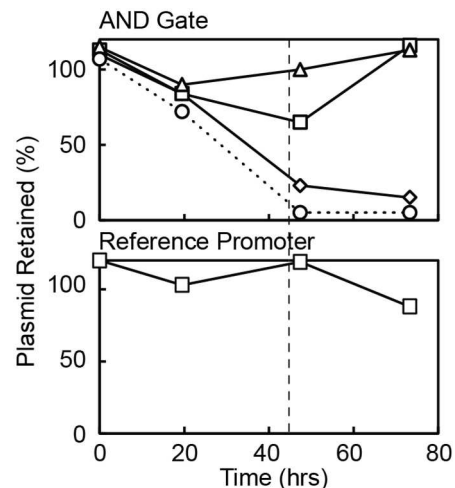
V. Plasmid retention in the 10 L bioreactor

In the 10 L bioreactor, the fluorescence from the AND gate declines late in fermentation (Figures 7, S7). The loss of plasmids is a common problem in fermentation. In order to determine the contribution of plasmid loss to circuit failure, plasmid retention was quantified. To assess plasmid loss during fermentation, we plated samples from different time points of Runs # 9 and 10 on selective plates (Figure S8). At each time point, a sample of culture was taken, diluted, and plated on 2xYT agar containing either no antibiotic, single antibiotics, or combinations of antibiotics. Percent plasmid

retained at each time point is calculated by dividing the number of colonies growing on a selective plate by the number of colonies growing on a nonselective plate at the same dilution.

The AND gate consists of three plasmids. The loss of any one of these three plasmids would result in the inability to perform the AND function. By 48 hours, almost all cells assayed had lost at least one essential plasmid (Figure S8). The loss of these plasmids is most likely due to the loss of selective pressure to retain the plasmids following fast degradation of antibiotics at high cell densities.⁵ The CamR plasmid (pAC_SalSer914), which expresses the supD tRNA, is particularly unstable. This suggests that there is selective pressure against producing supD. However, the reference plasmid pFM46 and the AmpR plasmid in the AND gate (pBR939b), both of which produce GFP reporter, were stably retained through the end of fermentation.

Figure S8: Plasmid loss in the AND gate and reference plasmid strains in the 10 L bioreactor. Retention of the plasmids composing an AND gate and the reference plasmid pFM46 were measured in *E. coli* DS68637 at several time points throughout Runs # 9 and 10, respectively. The percent of cells retaining KanR (squares), CamR (diamonds), AmpR (triangles), and all plasmids (circles) is plotted. The dotted line marks the time at which the feed rate was switched from exponentially growing to constant.



VI. Relative Expression Units (REUs) Conversions

In Figure 8 of this work, we use relative expression units (REUs) to compare expression of fluorescent reporter protein between conditions. REU's are simply the result of multiplying the raw fluorescence data produced by each instrument by a linear factor (Figure S9A). This linear factor relates the amount of fluorescent protein expression of the experimental construct to that of a standard plasmid in the given condition. We use REU instead of the more widely-accepted RPU (Relative Promoter Units) used by Kelly and coworkers because differences in the plasmid backbones, fluorescent proteins, and regulation make calculation of RPU as defined by Kelly et al. impossible.^{9,10,11} Instead, we use the relative amount of reporter protein produced by Kelly et al.'s standard plasmid to compare expression levels between contexts.

To determine REU conversion factors, we measured a strain carrying a reference plasmid pFM46 in parallel with AND gate strains in all contexts. In the first conversion step (Figure S-9B), we normalize the GFP expression of the AND gate reporter plasmid (pBR939b) by the GFP expression of pFM46. Because the raw arbitrary fluorescence unit reported by each instrument is different, the initial conversion factor changes with context and instrument. In shake flasks, this initial conversion factor (0.00012) is 1 divided by the geometric mean of the fluorescence of the pFM46 construct in DS68637[†] grown in minimal media, measured at 24 hours. In the microreactor, the initial conversion factor (0.41) is 1 divided by the mean arbitrary fluorescence of the pFM46 construct in DS68637 between 15 and 40 hours, the time period in which the fluorescence signal was stable. In the 10 L fermentor, the initial conversion factor (0.0067) is 1 divided by the mean fluorescence value of the pFM46 construct in DS68637 across the entire fermentation. In the second conversion (Figure S9C), we account for some differences between pBR939b and pFM46. Because effective comparison of expression can only be done within the framework of the same fluorescent protein, we took into account the contribution of the LVA (ssrA) tag on the GFP of pBR939b. The value of this conversion is reported as the average ratio of the

GFP fluorescence of pFM46 to J23102.egfp.LVA (0.082) in DS68637 during exponential growth. Because the LVA tag dramatically reduces the amount of GFP in the cells, we had to use a much stronger RBS similar to the one in pBR939bto achieve measurable levels of GFP. Therefore, this conversion also accounts for the change in RBS from pFM46 to pBR939b. One should note, however, that this conversion does not account for differences in copy number (p15A vs. pMB1) or other differences between the plasmids. Finally, we compared the expression of pFM46 to that of Kelly et al. using the average J23102 RPU to J23101 RPU ratio reported in that work (0.86).⁸ The final conversion factors are calculated as follows: for shake flasks, $8.46E^{-6}$ REU/au= 0.00012 x 0.082 x 0.86, for the microreactor, $2.89E^{-2}$ REU/au= 0.41 x 0.082 x 0.86, and for the 10 L fermentor, $4.72E^{-2}$ REU/au= 0.0067 x 0.082 x 0.86. Dividing by these respective factors converts REU in Figure 8 back to raw arbitrary fluorescence units measured by each instrument.

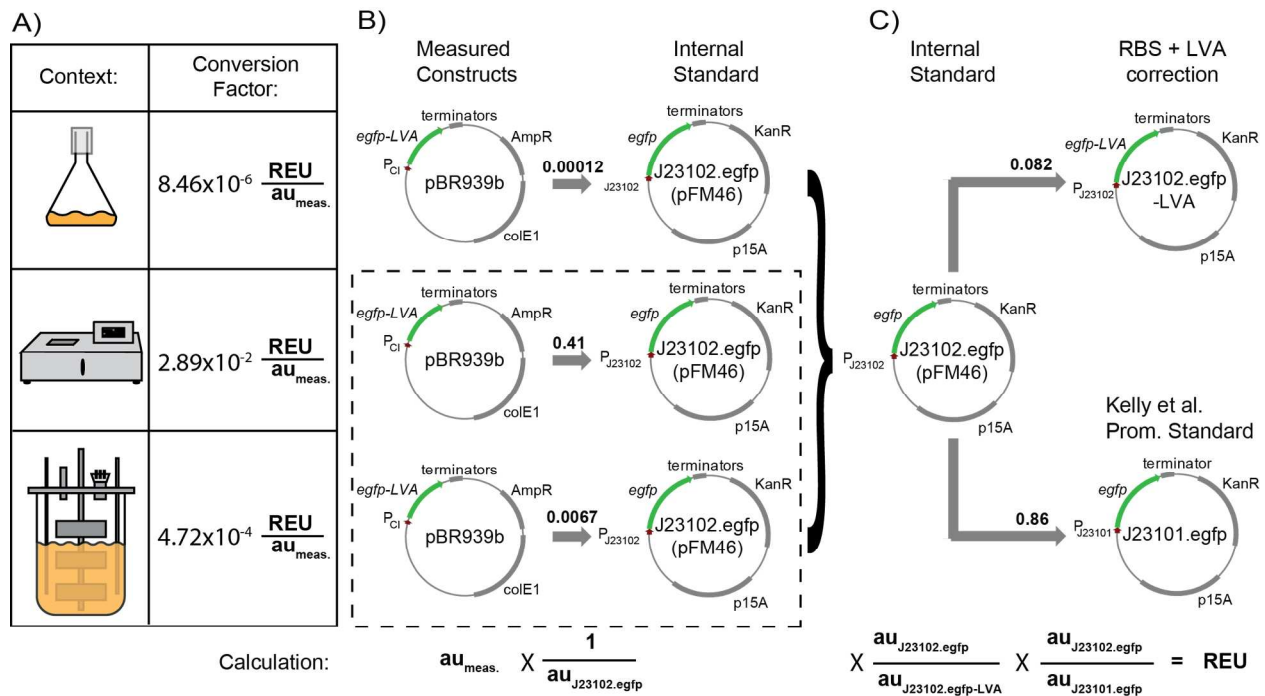


Figure S9: Conversion of arbitrary units into relative expression units (REU) for AND gate comparisons. The schematic illustrates the conversion from raw arbitrary fluorescence units to REU. A) The table summarizes the final calculated conversion factors in each measured context. B) The AND gate output plasmid (pBR939b) is measured in parallel with the reference plasmid pFM46 (designated J23102.egfp to highlight component similarities with other plasmids). The experimental fluorescence measurements were normalized by the fluorescence of this reference plasmid. The boxed constructs were measured at DSM and unboxed plasmids were measured at UCSF. C) The reference plasmid pFM46 was measured in parallel with a similar plasmid carrying a stronger RBS and LVA-tagged GFP (J23102.egfp-LVA) to account for the effects of the LVA tag on the GFP expressed by pBR939b. The promoter J23102 of the reference plasmid pFM46, which is identical to the Kelly et al. standard plasmid except for the promoter, was reported to be 0.86 the strength of J23101. Due to the similarity of these plasmids (only a few base pairs change within the promoter), this ratio is expected to be independent of context. The calculations at the bottom reflect the corresponding plasmid ratios above.

VII. Variations and Parameters of Individual 10 L Bioreactor Runs

All 10 L bioreactor runs were carried out as described in the Methods section in the main text, and any variation from this protocol is given in each series' section below. Differences in media composition and fermentation parameters between each run are summarized in Table S1. Runs #1-3 refer to the experiments in Figure 7. Runs #4-5 refer to data in Figure S7A. Runs #6-8 refer to the AND gates in Figure 8. Runs #9 and 10 refer to the AND gate and reference plasmid data in Figure S7B, respectively. Runs within the same series (#1,2,3, #4,5, #6,7,8, and #9,10) are grouped together spacially in Table S1 and Figure S10.

Table S1: Detailed parameters of runs in the 10 L bioreactor

Run	#1	#2	#3	#4	#5	#6	#7	#8	#9	#10
Circuit	AND RBS _B			AND RBS _C		AND RBS _B	AND RBS _C	AND RBS _D	AND RBS _B	Ref. J23102
Strain	<i>E. coli</i> DH10B			<i>E. coli</i> DS68637		<i>E. coli</i> DS68637		<i>E. coli</i> DS68637		
Batch	4 g/kg glucose+10 g/kg YE+ 5 g/kg (NH ₄) ₂ SO ₄ +0.5 g/kg leucine			4 g/kg glucose+10 g/kg YE+ 2 g/kg (NH ₄) ₂ SO ₄		4 g/kg glucose +10 g/kg YE+ 2 g/kg (NH ₄) ₂ SO ₄		4 g/kg glucose +10 g/kg YE+ 2 g/kg (NH ₄) ₂ SO ₄		
Feed	100 g/kg YE +250 g/kg glucose +2.5 g/kg leucine	20 g/kg YE 250 g/kg glucose 2.5 g/kg leucine	0 g/kg YE/ +250 g/kg glucose +2.5 g/kg leucine	400 g/kg glucose +20 g/kg YE	400 g/kg glucose	400g/kg glucose		400g/kg glucose		
pH titrants	2-fold diluted 25% NH ₃ solution			10% NH ₃ solution		10% NH ₃ solution, 4N H ₂ SO ₄		10% NH ₃ solution, 4N H ₂ SO ₄		
Feed Rate	Exponential feed profile during 60 h programmed into computer. Based on $\mu = 0.05 \text{ h}^{-1}$, starts at 4 g/h, feedmax 80.3 g/h.			Exponential feed profile during 60 h programmed into computer in table. Based on $\mu = 0.05 \text{ h}^{-1}$, final rate 45 g/h, duration 60 h (starts at 2.24 g/h). From 60 h onwards 45 g/h.		Exponential feed profile during 60 h programmed into computer in table. Based on $\mu = 0.05 \text{ h}^{-1}$, final rate 45 g/h, duration 42 h (starts at 5.5 g/h). From 42 h onwards 45 g/h.		Exponential feed profile during 60 h programmed into computer in table. Based on $\mu = 0.05 \text{ h}^{-1}$, final rate 45 g/h, duration 42 h (starts at 5.5 g/h) From 42 h onwards 45 g/h.		
Time of induction	~ 48 hrs			24 hr	22 hrs (Salicylate) and 26 hrs (Arabinose)	22 hrs (Salicylate) and 26 hrs (Arabinose)		22 hrs (Arabinose) and 25 hrs (Salicylate)..		
Airflow	5 nL/min			2-4 hrs: headspace aeration at 2 nL/min. >4 hrs: submerged aeration 4 nL/min		0-6hrs: 2 nL/min >6hrs: 4 nL/min		0-6hrs: 2 nL/min >6hrs: 4 nL/min		

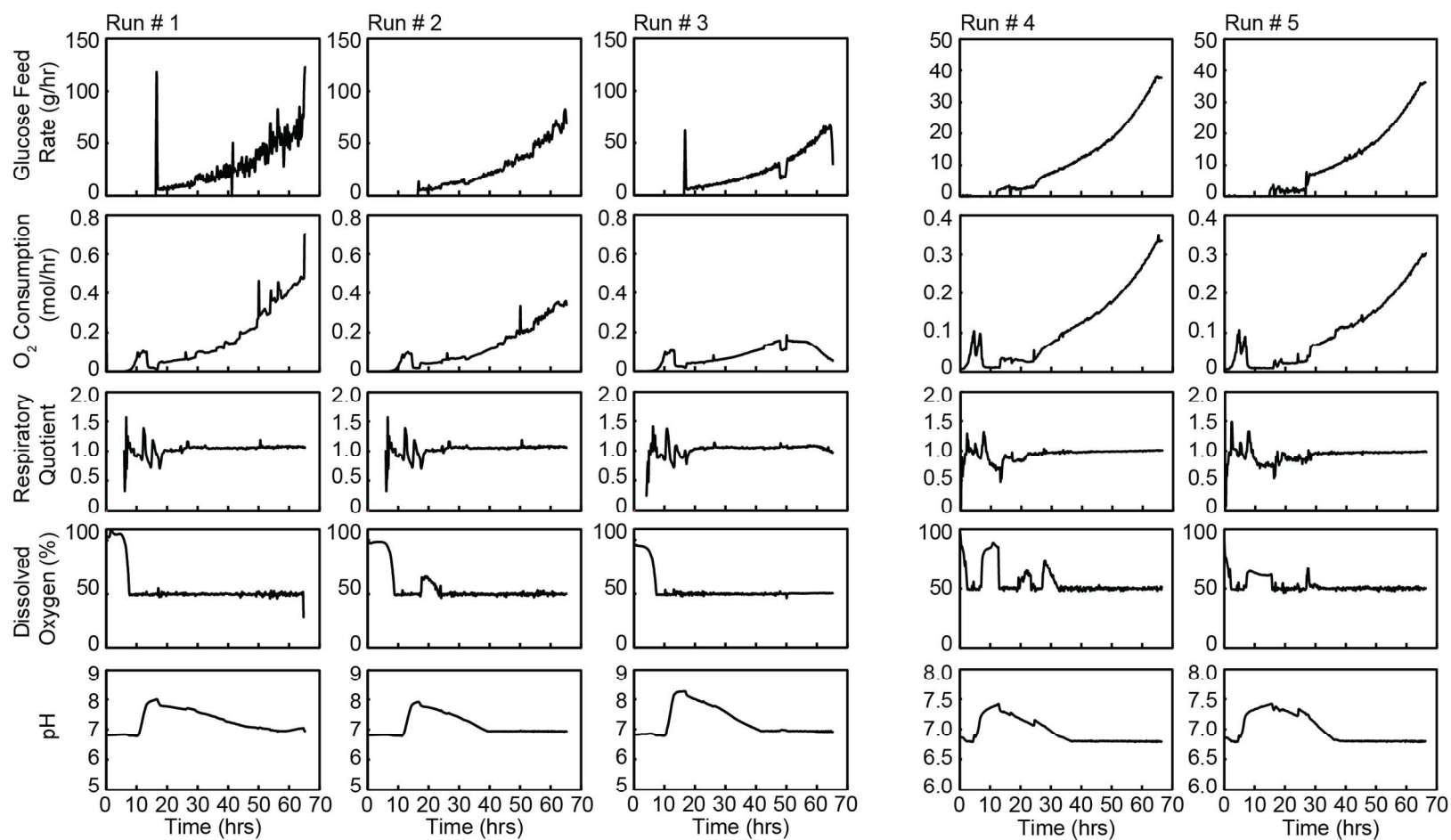


Figure S10: Detailed data recorded from the 10 L bioreactor runs. Glucose feed is calculated and controlled by the central computer and monitored by feed weight. Variation in glucose feed in Run #1 was due to a faulty pump. Molar O_2 consumption and CO_2 production rates are monitored over time by mass spectrometry and are equal when the respiratory quotient (RQ) equals 1. In most fermentations, the RQ stabilizes at 1 following the start of the exponential glucose feed. The dissolved oxygen (DO) is monitored by an oxygen probe and controlled by impeller speed and airflow. DO is initially kept near 100% during batch phase and then drops to 50% throughout exponential feeding. Variation in DO throughout fermentation was due to occasional problems with the oxygen probe. The pH of each culture is monitored by an electrode in real time and confirmed off-line by an independent electrode following sampling.

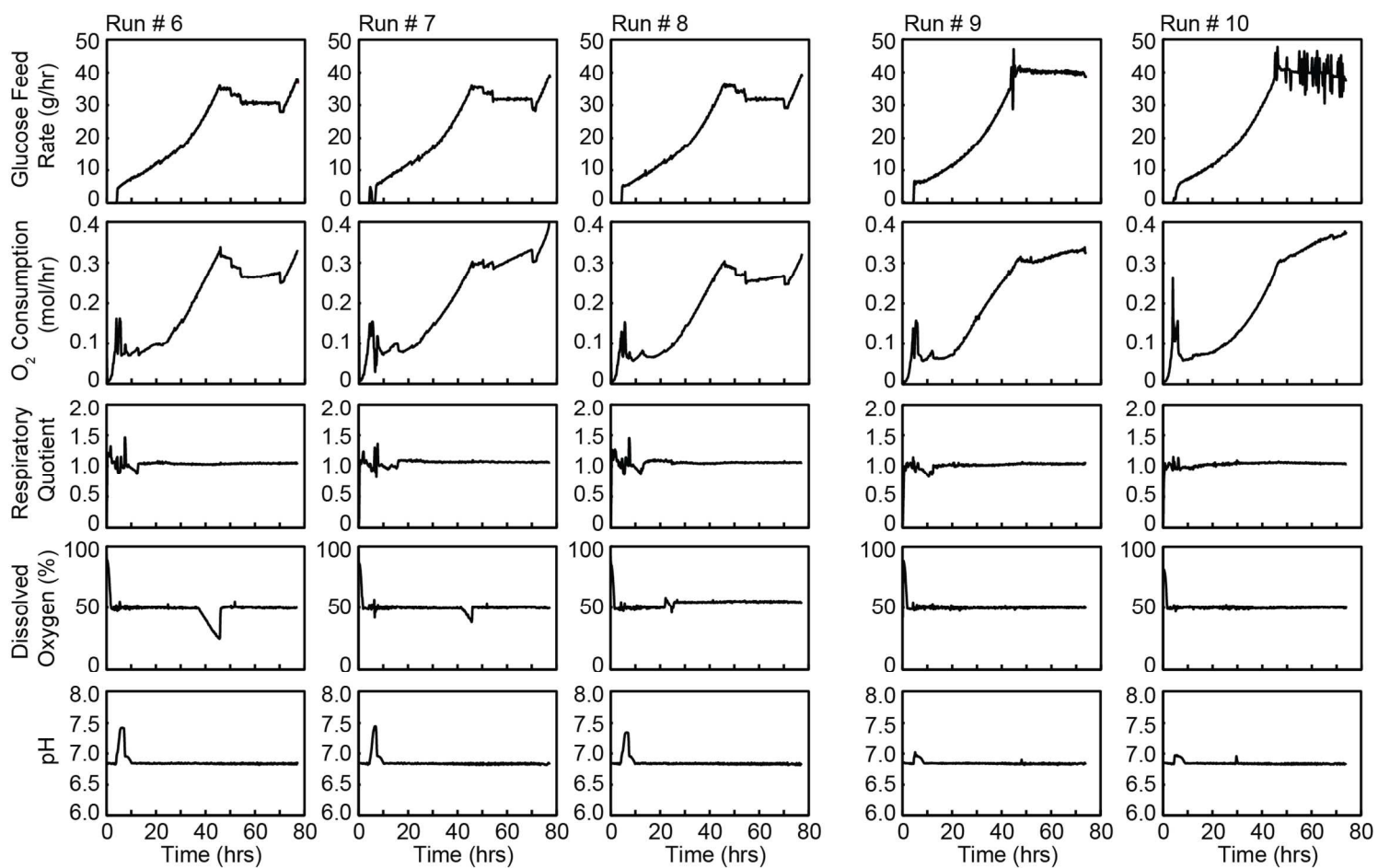


Figure S10 (continued)

VII.A. Runs #1-3: AND gate in *E. coli* DH10B with different amounts of yeast extract.

The purpose of this series was to test the AND gate in *E. coli* DH10B in bioreactor conditions with different concentrations of yeast extract (100, 20, and 0 g/kg) in the feed. The addition of large amounts of yeast extract to the feed required customizing some of the parameters of the fermentation. To dissolve sufficient yeast extract in the feed, the glucose concentration in the feed had to be lowered (Table S1). Therefore, higher feed rates had to be programmed into the control computer to maintain the same glucose-limited growth rate in the culture. Additionally, the dissolved oxygen was maintained at 100% longer throughout batch growth to aid in the growth of the culture. Additional ammonium sulfate and leucine were also added to the batch to support growth of the *E. coli* DH10B strain.

Addition of yeast extract to the feed changed both AND gate performance and growth characteristics of the cultures during fermentation. The AND gate functioned only in the culture containing 100 g/kg yeast extract in the feed (Figure 6B). Also, oxygen consumption late in the run increased with increased amounts of yeast extract in the feed (Figure S10). Although the feed rates of all fermentations increased identically, the feed with added yeast extract provided more nutrition per gram of feed. This is why the fermentations with more yeast extract in the feed showed higher rates of oxygen consumption. In contrast, the culture with no yeast extract in the feed displayed much slower growth in oxygen consumption followed by a decrease of oxygen consumption after 56 hours (Figure S10). These trends are most likely due to the availability of nutrients late in fermentation. When supplemental nutrients from the yeast extract are exhausted late in fermentation, the culture is forced to slow its metabolic rate. However, although oxygen consumption of the fermentation with 100 g/kg of yeast extract in the feed continues to increase, the fluorescence signal of the AND gate decreases by the end of the run (Figure 6B). Plasmid loss was not assessed in these fermentations.

VII.B. Runs #4-5: AND gate in *E. coli* DS68637 with different amounts of yeast extract

The AND gate was observed to perform well in *E. coli* DS68637 without addition of yeast extract to the media in shake flasks (Figure S7A). To test if this functional independence to media was consistent for fermentation conditions, we tested AND gate function in *E. coli* DS68637 during fermentation with different amounts of yeast extract in the media.

For this fermentation, smaller amounts of yeast extract (20 g/kg) were added to the feed, and therefore the glucose concentration did not need to be reduced. As a consequence, feed rate was also reduced compared to Runs #1-3. Since *E. coli* DS68637 is not auxotrophic, no additional supplements were added to either the batch or the feed.

VII.C. Run #6-8: AND gate RBS variants in *E. coli* DS68637

To test if the choice of optimal RBS in an AND gate is consistent between shake flask and fermentation conditions, we grew three different RBS variants (RBS_B, RBS_C, RBS_D) of the AND gate in fermentation conditions. None of the fermentations in this series contained any yeast extract in the feed. The final feed profile was therefore different than in previous fermentations, although it was identical to the first two days of the feed profile of Runs #4-5. All three gates were first induced with salicylate and then with arabinose 4 hours later. More time points were sampled so as to assess AND gate function more fully throughout fermentation. GFP *visibly* accumulated in RBS_B and RBS_C AND gate variants only a few hours after full induction. After 45 hours, the feed rate was held constant and adjusted twice. At ~72 hours, the exponential feed was again increased to test whether GFP production could be recovered by feeding the cells.

VII.D. Run #9-10: AND gate and the reference plasmid in *E. coli* DS68637

The final series of runs aimed to compare the performance of the RBS_B AND gate and a reference plasmid *E. coli* DS68637. The reference plasmid (pFM46) consists of a strong, constitutively active promoter (J23102) and RBS (B0032) driving expression of GFP from a p15A origin, Kan^R plasmid (Table S2, S3).⁸ This standard plasmid was expected to maintain approximately the same level of expression throughout fermentation, with the only variability in observed GFP expression due to innate changes in expression and metabolism. Comparing the fermentations of the AND gates to the fermentation of this plasmid enabled us to normalize by these innate changes in expression and metabolism and make a more informative comparison of circuit performance. These fermentations were carried out identically to runs #6-8, except that induction was done first with arabinose, followed by salicylate (AND gate) induction 3 hours later. Inducing first with arabinose tested the alternate state of the AND gate and showed that the gate turned on with only arabinose inducer.

VIII. Genetic Parts and Plasmids

Genetic parts and plasmids were derived from previous work^{1,2,8} and the Registry of Standard Biological Parts (http://partsregistry.org/Main_Page). Table S2 summarizes all the RBSs used in this work, their predicted ΔG_{tot} according to the RBS calculator², and the plasmid that uses them. Table S3 provides a concise description of all the plasmids used in this work and the GenBank accession # through which the entire annotated sequence of each plasmid can be accessed via the internet.

Table S2: RBS Sequences used in this work

RBS Name	RBS Sequence	Predicted ΔG_{tot}	Plasmid
RBS _A	ATAGATCACTCTTCCCCAGGAGCACTAAGTCCAC	-1.48	pFM163
RBS _B	CTGGACAACACCGACGAACCTGGAGCCTCCGGC	0.60	pFM161
RBS _C	TAACCTAATCTTAAAAACCCGCACAAAGCAAAC	2.18	pFM159
RBS _D	TACATTCACCTACCTGCAAAGACACATCGATAACG	7.35	pFM160
FwEng 1*	TTCTAGAAAACAAAATGAGGAGGTACTGAGATGGCGAGCTC	-7.09	pFM169
FwEng 2*	TTCTAGAAAGCTGATAAGGAGGTATAACGATGGCGAGCTC	-6.89	pFM170
FwEng 5*	TTCTAGACTGGTGAGGAGGTGAGAATGGCGAGCTC	-5.37	pFM171
FwEng 6*	TTCTAGAAAAGTAAGGAGGCCGCGCTATGGCGAGCTC	-4.89	pFM172
FwEng 11*	TTCTAGAAGCGAGGAGGCCAGTCGATGGCGAGCTC	-2.58	pFM173
FwEng 14*	TTCTAGAGGAGGATAACCACTATGGCGAGCTC	-2.12	pFM174

*These RBSs were previously annotated as part of the Forward Engineering series in Salis, et al (2009).²

Table S3: Summary of plasmids used in this work

Name	Description	Ori	Ab. Res	Accession #
pFM46	Standard promoter BBa_J23102, RBS BBa_B0032, driving EGFP (BBa_E0040) ⁸	p15A	Kan	JQ394801
pFM159	pBAD promoter, RBS _C , driving T7RNAP (same as pBACr-AraT7940 ^{1,2} with RBS#4)	R6K	Kan	JQ394800*
pFM160	pBAD promoter, RBS _D , driving T7RNAP (same as pBACr-AraT7940 ^{1,2} with RBS#8)	R6K	Kan	JQ394800*
pFM161	pBAD promoter, RBS _B , driving T7RNAP (same as pBACr-AraT7940 ^{1,2} with RBS#9)	R6K	Kan	JQ394800
pFM163	pBAD promoter, RBS _A , driving T7RNAP (same as pBACr-AraT7940 ^{1,2} with RBS#11)	R6K	Kan	JQ394800*
pFM169	Promoter BBa_J23100 and RBS	ColE1	Cam	JQ394804

	FwEng1driving mRFP1 (codon modified BBa_E1010) ²			
pFM170	Promoter BBa_J23100 and RBS FwEng2 driving mRFP1 (codon modified BBa_E1010) ²	ColE1	Cam	JQ394804 [†]
pFM171	Promoter BBa_J23100 and RBS FwEng5 driving mRFP1 (codon modified BBa_E1010) ²	ColE1	Cam	JQ394804 [†]
pFM172	Promoter BBa_J23100 and RBS FwEng6 driving mRFP1 (codon modified BBa_E1010) ²	ColE1	Cam	JQ394804 [†]
pFM173	Promoter BBa_J23100 and RBS FwEng11 driving mRFP1 (codon modified BBa_E1010) ²	ColE1	Cam	JQ394804 [†]
pFM174	Promoter BBa_J23100 and RBS FwEng14 driving mRFP1 (codon modified BBa_E1010) ²	ColE1	Cam	JQ394804 [†]
pBR939b ^{1,2}	T7 promoter driving GFP	pMB1	Amp	JQ394798
pAC_SalSer914 ^{1,2}	Psal driving supD tRNA	p15A	Cam	JQ394799
pNOR10-20 ⁴	PBad and Ptet (BBa_R0040) driving CI expression. Encodes AraC and TetR.	ColE1	Cam	JQ394802
pCI-YFP ⁴	PCI driving YFP expression.	p15A	Kan	JQ394803

* The RBS in this construct should be replaced with the one in JQ394800 for the accurate sequence.

[†] The RBS in this construct should be replaced with the one in JQ394804 for the accurate sequence.

IX. Supplementary References

1. Anderson, J.C., Voigt, C.A., and A.P. Arkin (2007) Environmental signal integration by a modular AND gate. *Molecular Systems Biology* 3: 133.
2. Salis, H.M., Mirsky, E.A., and C.A. Voigt (2009) Automated Design of Synthetic Ribosome Binding Sites to Precisely Control Protein Expression. *Nat. Biotech.* 27(10), 946-950.
3. Peccoud, J. et al. (2011) Essential information for synthetic DNA sequences. *Nat. Biotech.* 29 (1), 22.
4. Tamsir, A., Tabor, J., and C.A. Voigt (2011) Robust multicellular computing using genetically-encoded NOR gates and chemical 'wires'. *Nature* 212 (469), 212-215.
5. Andersson, L., Yang, S., Neubauer, P., and S-O. Enfors (1996) Impact of plasmid presence and induction on cellular responses in fed batch cultures of *Escherichia coli*. *J. Biotechnology* 46,255-263.
6. Friehs, C. (2004) Plasmid Copy Number and Plasmid Stability. *Adv. Biochem. Eng. Biotechnol.* 86, 47-82.
7. Huber, R., Roth, S., Rahmen, N., and J. Büchs (2011) Utilizing high-throughput experimentation to enhance specific productivity of an *E.coli* T7 expression system by phosphate limitation. *BMC Biotechnol.* 11, 1-11.
8. Kelly, J.R., Rubin, A.J., Davis, J.H., Ajo-Franklin, C.M., Cumbers, J., Czar, M.J., de Mora, K., Gliberman, A.L., Monie, D.D., and D. Endy (2009) Measuring the activity of BioBrick promoters using an in vivo reference standard. *J. Biol. Eng.* 3,1-13.
9. Temme, K., Zhao, D., and C.A.Voigt (2012) Refactoring the nitrogen fixation gene cluster from *Klebsiella oxytoca*. *Proc. Natl. Acad. Sci.* 109(18), 7085-7090.
10. Zucca, S., Pasotti, L, Mazzini, G., De Angelis M.G.C., and P. Magni (2012) Characterization of an inducible promoter in different DNA copy number conditions. *BMC Bioinformatics* 13, S11.
11. Davis, J.H., Rubin, A.J., and R.T. Sauer (2011) Design, construction, and characterization of a set of insulated bacterial promoters. *Nucleic Acids Res.* 39(3): 1131-1141.